2011 IEEE/RSJ International Conference on
Intelligent Robots and Systems
September 25-30, 2011. San Francisco, CA, USA

Toward Simpler Models of Bending Sheet Joints

Lael U. Odhner, *Member, IEEE*, and Aaron M. Dollar, *Member, IEEE*

Abstract— **Sheet hinges, thin flexures that are rigid in the plane but which can bend freely, are common in stamped and lithographically manufactured devices. The behavior of these machine elements as joints in a robot is difficult to model because they are two-dimensional continuum elastic bodies that admit three-dimensional motion and twisting. This paper presents a parametric modeling technique that can be used to accurately predict elastic behavior of sheet hinges in three dimensions. Parameterized backbone curves can be used to represent ruled surface bending in a fashion that implicitly accounts for some of the complex boundary conditions imposed on typical sheet hinges. Approximate methods of integrating the non-commutative equations defining the sheet hinge backbone curves will be discussed, demonstrating acceptable trade-offs between accuracy and representational simplicity in overall model performance.**

I. Introduction

ELASTIC hinges made out of thin bending sheets are simple, effective joint mechanisms for robots, particularly those manufactured by layered or lithographic processes, or made out of folded sheets of material. The geometric simplicity of sheet hinges makes them extremely scalable, so that robots on the macro-scale [1], meso-scale [2, 3], or macro-scale [4, 5] can obtain repeatable, low-backlash motion with little or no friction.

One challenge facing the designers of robots having elastic members of any kind is the need for a low-dimensional representation of robot configuration. Most classical modeling and control techniques assume that the configuration of a robot can be entirely described by its joints via a vector of joint angles or displacements, and that the Jacobians and Hessians used to analyze the kinetostatics and dynamics of the robot are easy to compute from the joint configuration vector. In contrast, continuum bodies such as sheets can deform in a wide variety of ways, including coupled translation and rotation, or bending about multiple axes, as shown in Fig. 1. In order to reap the benefits of classical analytical techniques for robots, a joint model is needed that can, with a small set of parameters per joint, reproduce the range of motions caused by elastic deformation. Additionally, the energy associated with any deformation must be modeled, in order to accurately predict elastic forces and deflection of the joint under load.

If only planar motion is considered, a sheet hinge can be passably approximated by the large-deformation Euler-Bernoulli equation, and many approximations of this and other derivative beam models have been made for describing flexure hinges. The method of finite elements has been proposed as a means of generating a parametric configuration for flexible robots [6], although the models produced in this manner often have many parameters and become computationally intensive to solve. The Pseudo-Rigid Body technique, fitting a linkage with nonlinear springs to the flexure behavior by regression, can also produce parameterized models of beam bending that characterize the behavior of elastic bodies for a limited range of motion [7, 8]. The authors recently published a more general-purpose model, called the Smooth Curvature Model, which accurately predicts large-deformation in-plane beam bending under arbitrarily oriented end loads using only three parameters [9].

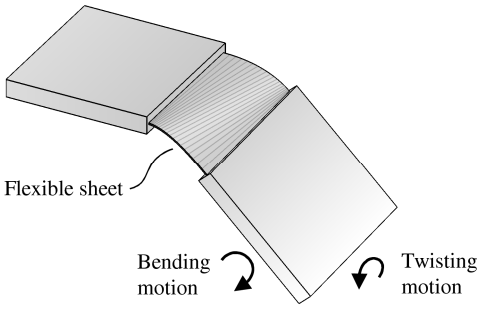

Fig. 1. Sheet of elastic material are often used as a joints between two rigid bodies. However, the possible motions of sheet hinges are more complex than those of a standard revolute joint.

Predicting the true three-dimensional behavior of bending sheets is more difficult. Unlike the better-understood case of slender rods [10], bending sheets do not locally yield in torsion to produce three-dimensional deformation. Instead, three-dimensional deformation is produced as a result of varying rotations in the plane of the sheet hinge. In this paper, we will derive a new, low-dimensional parametric model of sheet bending based on the elastic mechanics of developable strips [11]. The principal curvature along the centerline of the sheet hinge, and the angle at which the sheet is bent locally will be represented as superpositions of polynomial modes, under the assumption that the backbone curve of a bending sheet will be smooth at equilibrium. The coefficients of the polynomial terms can be used as a coordinate basis for describing the sheet's continuum configuration, and can also be used to compute Jacobians and Hessians of robot kinematics in terms of these coordinates.

This work was supported in part by National Science Foundation grant IIS-0952856 and by DARPA ARM-H, grant W91CRB-10-C-0141.

L.U. Odhner and A.M. Dollar are with the Department of Mechanical Engineering and Materials Science, Yale University, New Haven, CT USA (e-mail: {lael.odhner, aaron.dollar}@yale.edu).

We will proceed in the following order: First, the basic mechanics of bending in a developable sheet or strip will be reviewed, along with a discussion of the physical constraints imposed on a typical sheet hinge. Parameterizations of these mechanics using polynomial mode shapes will be discussed, followed by an overview of problems surrounding numerical integration. The accuracy of solutions obtained by these smooth curvature models will be discussed by examining the *a posteriori* prediction of elastic forces in a sheet for any equilibrium configuration.

II. The Mechanics of Bending Sheets

A joint, in the abstract sense, is a way of describing the relationship between two rigid bodies via a homogeneous transformation matrix, $\mathbf{G}(\vec{q})$, as a function of some joint parameter or parameters, $\vec{q}$. Additionally, any energy associated with the motion of the joint, such as elastic energy, must be described by some function, $V(\vec{q})$, to ensure that elastic forces are accurately represented. In this section, constitutive expressions will be found for $\mathbf{G}$ and V in terms of the continuum configuration of a bending sheet hinge. Because bending sheets are developable surfaces, the shape of the joint and the energy associated with joint motion can be written as functions of the magnitude and orientation of the principal curvature along the sheet's backbone, a parametric space curve running down the center of the hinge. Some of the physical intuition behind the structure of $\mathbf{G}$ and V will be discussed. After the underlying constitutive behavior of bending sheets or strips is understood, focus will turn to the problem of producing an approximate parametric model of joint motion.

A. The Kinematics of Sheet Bending

A sheet of material that is too stiff to deform in the plane but capable of bending is often referred to as a ruled or developable surface. The internal constraints imposed by such shapes force the bending curvature of the surface to be simple – that is, it is possible to draw straight lines of zero curvature through any point on the surface that lies completely along the surface, resulting in the local area being equivalent to a section of a cone. A side effect of this constraint is that the deformation of a whole sheet can be described by the bending occurring on a single backbone drawn across the sheet, as shown in Fig. 2. Such a curve, running end-to-end between two links of a robot, can be parameterized in terms of its arc length, $s \in [0, L]$. The local coordinate frame of this backbone curve forms a rotation matrix, $\mathbf{R}$, whose local axes are depicted in Fig. 2, with x tangent to the backbone and z perpendicular to the backbone but along the sheet. Again, there is assumed to be no extension or shearing in the plane, only bending of magnitude $\kappa(s)$ about a principal axis of rotation at some angle, $\theta(s)$, as shown in Fig. 3. The change in $\mathbf{R}$ as a function of s is given by the well-known relationship:

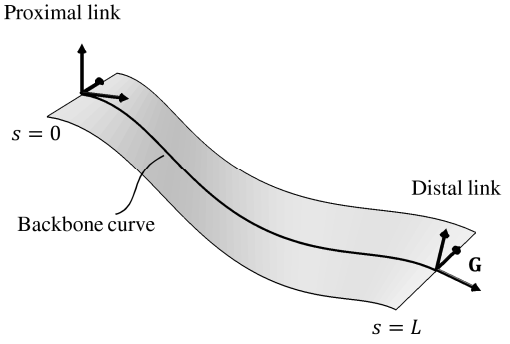

Fig. 2. The backbone curve of a flexible strip is the curve running along the center line of the strip from one end to the other. The end-to-end transformation along the curve can be represented with a homogeneous transformation matrix, **G**.

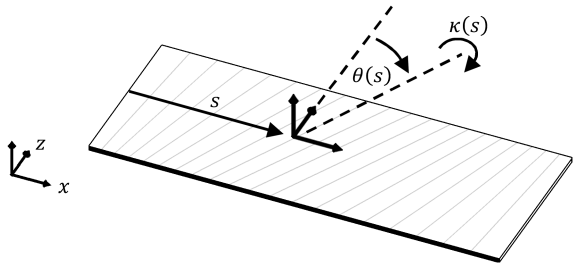

Fig. 3. Local evolution of the backbone curve at a point s is defined by an instantaneous rotation of magnitude $\kappa(s)$ along an axis at an angle $\theta(s)$ to the y axis in body coordinates.

$$\frac{d\mathbf{R}}{ds} = \mathbf{R}(s)\boldsymbol{\Omega}(s) \tag{1}$$

The matrix $\boldsymbol{\Omega}(s)$ is the skew-symmetric form of the rotation rate vector,

$$\boldsymbol{\Omega}(s) = \kappa(s)\begin{bmatrix} 0 & -\cos\theta(s) & 0 \\ \cos\theta(s) & 0 & -\sin\theta(s) \\ 0 & \sin\theta(s) & 0 \end{bmatrix} \tag{2}$$

The evolution of the backbone position, $\vec{x}$, is also defined in terms of the local coordinate axes as described by $\mathbf{R}(s)$,

$$\frac{d\vec{x}}{ds} = \mathbf{R}(s)\begin{bmatrix}1\\0\\0\end{bmatrix} = \mathbf{R}(s)\vec{v}(s) \tag{3}$$

The body frame velocity, $\vec{v}(s)$, corresponds to moving at a constant rate down the backbone curve. Put together, (1) and (3) describe the shape of the backbone curve as a linear, time-varying (LTV) differential equation in $SE(3)$,

$$\frac{d}{ds}\begin{bmatrix}\mathbf{R}(s) & \vec{x}(s)\\ 0_{1\times3} & 1\end{bmatrix} = \begin{bmatrix}\mathbf{R}(s) & \vec{x}(s)\\ 0_{1\times3} & 1\end{bmatrix}\begin{bmatrix}\boldsymbol{\Omega}(s) & \vec{v}(s)\\ 0_{1\times3} & 0\end{bmatrix} \tag{4}$$

Because the backbone curve runs between the edges of the sheet connecting two robot links, solving (4) on $[0, L]$ can be used to calculate the kinematic relationship, $\mathbf{G}$, between the links. Thus, the same continuum configuration describing the shape of the whole sheet ($\kappa(s)$ and $\theta(s)$) also describes the joint kinematics. It bears mentioning here that although $\boldsymbol{\Omega}$ and $\vec{v}$ are exponential coordinates describing the local behavior of the backbone curve, they cannot be used as they

are in typical screw-based joint models [12]. The LTV system in (4) is non-commutative, so matrix exponentiation cannot be used to solve for **G**. More general methods of solution will be discussed in further sections.

B. The Energy of a Bending Strip

We now turn from discussion of the sheet hinge's shape to the elastic energy stored in any deformed configuration. The bending energy of a sheet or strip is locally defined by the curvature about both axes in the plane, κ_x and κ_z:

$$V = \frac{h^3 E}{12(1-\nu^2)} \int_0^L \int_0^w (\kappa_x^2 + \kappa_z^2) dA \tag{5}$$

The limits of integration correspond to the length of the strip, L, and the strip of the strip, w. Because of the geometric constraints on the curvature of a developable surface (it cannot have compound curvature), the curvature at any point on the strip can be defined in terms of the local curvature along the backbone curve [11]. The expression for energy is a path integral from $s = 0$ to L, and it is often written in terms of κ_x and κ_z along the backbone. By making the substitutions $\kappa_z = \kappa(s)\cos\theta(s)$ and $\kappa_x = \kappa(s)\sin\theta(s)$, it will be written as before in terms of the principal curvature and bending axis angle,

$$V = \frac{wh^3 E}{12(1-\nu^2)} \int_0^L \kappa(s)^2 S(\gamma) ds \tag{6}$$

$$\gamma = \frac{w}{2\cos^2\theta(s)} \frac{d\theta}{ds} \tag{7}$$

$$S(\gamma) = \frac{\log(1+\gamma) - \log(1-\gamma)}{2\gamma} \tag{8}$$

The dimensionless group γ and the shape factor $S(\gamma)$ have been separated out of (6) because they capture several salient features of the bending energy of the strip. The first feature of note about the shape factor, plotted in Fig. 4, is that it will go to infinity as γ approaches either 1 or -1. This divergence can be explained by ascribing some real meaning to γ. A way of visualizing the local deformation of a sheet is to see a thin slice of the sheet as lying tangent to a cone, at an angle $\theta(s)$ from the backbone curve and a distance d from the

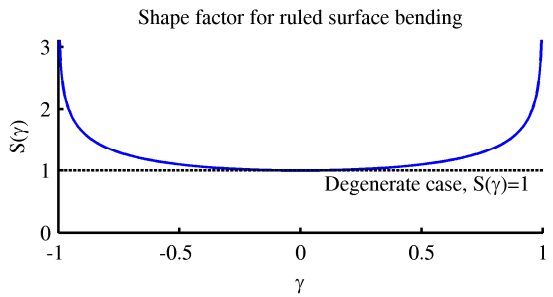

Fig. 4. The shape factor used to compute the energy of a bending strip is defined between -1 and 1, and is equal to 1 in the center, reducing the strip bending equation to the beam bending equation.

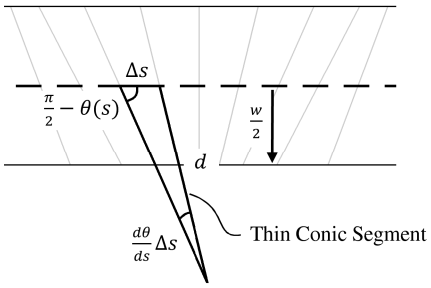

Fig. 5. The law of sines can be used to find the distance d from the backbone of the flexure to the point where two bending rules intersect, forming an angular section of a cone.

vertex of the cone, as illustrated in Fig. 5. The law of sines can be used to find d by considering the triangle shown in Fig. 4 for a small displacement Δs along the backbone,

$$\frac{d}{\sin\left(\frac{\pi}{2} - \theta(s)\right)} = \frac{\Delta s}{\sin\left(\frac{d\theta}{ds}\Delta s\right)} \tag{9}$$

It is possible to solve for d by taking the limit of (9) as Δs approaches 0,

$$d = \lim_{\Delta s \to 0} \frac{\Delta s \cos\theta(s)}{\sin\left(\frac{d\theta}{ds}\Delta s\right)} = \frac{\cos\theta(s)}{\frac{d\theta}{ds}} \tag{10}$$

The local energy of the strip at s is equal to the energy of the infinitesimal cone over the section tangent to backbone curve. At the vertex of the cone, the local bending energy becomes infinitely large, because the cone's radius of curvature goes to 0. Therefore, such a "vertex point" cannot exist on the edge or interior of the sheet. When a vertex exists at a distance $w/2$ from the backbone, the distance to the vertex is:

$$d\cos\theta(s) = \frac{\cos^2\theta(s)}{\frac{d\theta}{ds}} = \frac{w}{2} \tag{11}$$

Comparing (11) to (7), it is clear that there is a physical basis for asserting that γ will always lie between -1 and 1, namely, that the boundaries of a sheet can never be bent more tightly than a conical point.

C. An Important Degenerate Case

Another important property of the shape factor relates to the case when θ (and hence γ) are zero over the entire length of the strip. In this degenerate class of configurations, all bending will occur in the xy plane, and consequently (6) should reduce to the energy functional of a thin bending beam. This will be the case if the shape factor $S(0) = 1$,

$$V_{planar} = \frac{wh^3 E}{12(1-\nu^2)} \int_0^L \kappa(s)^2 ds \tag{12}$$

Unfortunately, $S(\gamma)$ is singular at $\gamma = 0$, because the numerator and denominator of the fraction in (8) both go to

zero. The limit of the expression can be shown by L'Hospital's rule to be 1. This kind of discontinuity, occurring in a common degenerate case, is problematic for numerical computation. One workaround is to approximate $S(\gamma)$ with a function that does not have a discontinuity at 0. This was accomplished by fitting a polynomial to $S(\gamma)$ using the Remez algorithm [13] on the interval between -0.1 and 0.1,

$$\hat{S}(\gamma) = \begin{cases} S(\gamma), & 0.1 < |\gamma| < 1 \\ 1 + 0.3353482\gamma^2, & |\gamma| \leq 0.1 \end{cases} \quad (13)$$

The residual error of (13) is within 2.53×10^{-6} at all points, and can be made as small as desired by changing the interval of the approximated function.

D. In Summary

So far, this section has defined a model that describes the configuration and elastic energy of a sheet hinge in terms of the principal curvature $\kappa(s)$ and the bending axis angle $\theta(s)$. The only assumption made thus far about these configuration functions is the differentiability of $\theta(s)$, which is needed in order to compute bending energy. In the upcoming section, these two arbitrary functions will be approximated with families of parametric functions, so that the configuration of the flexure can be discretized into a more convenient form.

III. Parameterizing the Sheet Hinge Model

So far, the model just introduced describes the configuration of a sheet hinge in terms of two arbitrary functions, $\kappa(s)$ and $\theta(s)$. What is really desired, however, is a parameterized description of the joint: some set of coordinates, $\vec{q}$, that provides a good-enough approximation of the physically obtainable flexure configurations. These coordinates can be used as joint variables, in the same sense as the angle of a revolute joint or the displacement of a prismatic joint. In this section, we will examine polynomials as a basis for describing hinge shape, motivated by the general observation that bending members loaded at the ends are smooth curves.

A. Representing Principal Curvature

The configuration of a sheet hinge deforming only in the plane is a function of the curvature, $\kappa(s)$, and modeling this case is equivalent to modeling an Euler-Bernoulli beam as a hinge. The authors have previously argued that in this planar case, a smooth approximation of curvature, such as a linear superposition of Legendre polynomials, will provide the most accurate and efficient parameterization of joint in this case [9]. Extending this notion to the more general problem of three-dimensional motion, the same approximation will be used for the principal curvature of a bending sheet,

$$\kappa(s, \vec{q}) = \frac{q_1}{L} + \frac{q_2}{L}\left(\frac{2s}{L} - 1\right) + \frac{q_3}{L}\left(\frac{6s^2}{L^2} - \frac{6s}{L} + 1\right) \quad (14)$$

The configuration variables $q_1 \ldots q_3$ are coefficients of Legendre polynomials, scaled to be orthogonal under convolution on the interval from 0 to L. This model accurately predicts tip deflection within 1% for bending in the plane at angles up to ± 90º [9].

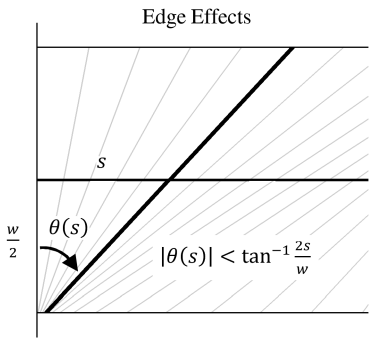

Fig. 6. The bending axis is constrained at the end of a strip by the fact that bending axes cannot intersect on the strip surface.

B. Parameterizing Bending Angle

Like the curvature of a bending sheet, the angle of the bending axis will also be a smooth function, because the limited domain of γ as shown in Fig. 4 imposes a constraint on the derivative of $\theta(s)$,

$$\left|\frac{d\theta}{ds}\right| < \frac{2\cos^2\theta(s)}{w} < \frac{2}{w} \quad (15)$$

Furthermore, the overall magnitude of $\theta(s)$ is dominated by strong boundary conditions at both ends. At the ends of the joint, the axis of bending in the sheet must be parallel to the edge of the much stiffer link. Because the axes of bending cannot intersect on the sheet, the sheet tends to form a frustum near the ends, so that the bending axes seem to pivot about one corner of the sheet, as illustrated in Fig. 6. This translates to an absolute constraint on the magnitude $\theta(s)$,

$$|\theta(s)| < \tan^{-1}\frac{2s}{w} \quad (16)$$

In a sheet having a relatively low aspect ratio, i.e. $L < w$, these two constraints will dominate the overall shape of the angular profile, so that the behavior of the whole angular profile can be predicted by two smooth modes corresponding to the angular constraints at each end. As with the curvature modes in (14), two polynomials will be used to represent these behaviors, mode that is symmetric about the center of the sheet, and one anti-symmetric mode,

$$\theta(s, \vec{q}) = q_4\frac{s}{L}\left(1 - \frac{s}{L}\right) + q_5\frac{s}{L}\left(1 - \frac{s}{L}\right)\left(\frac{2s}{L} - 1\right) \quad (17)$$

These modes have been constrained to implicitly account for the boundary conditions, $\theta(0) = \theta(L) = 0$.

C. Discussion

The five parameters $q_1 \ldots q_5$ approximately describe the shape and energy of a bending sheet over the typical regime of behaviors expected from bending sheets, based on reasonable assumptions about the range of motion and

aspect ratios of flexures typically encountered. While the use of only two modes for $\theta(s)$ seems low, it reflects the reality that most sheet hinges are designed to be short and wide, to minimize any twisting motion. In the upcoming section, this model will be used to derive Jacobians and Hessians of the joint motion with respect to this basis.

IV. Computing Joint Energy and Transformations

The primary computational problem associated with a joint model is in finding an efficient algorithm mapping some joint configuration, $\vec{q}$, onto the joint's homogeneous transformation, $\mathbf{G}(\vec{q})$, and the joint energy, $V(\vec{q})$. Because the sheet hinge model presented here involves three-dimensional rotations and translations, finding fast methods of integrating the kinematic equations is more difficult than in the case of planar bending hinges. However, due to the smoothness of the configuration functions $\kappa(s)$ and $\theta(s)$, inexpensive numerical integration techniques such as low-order fixed-step Runge-Kutta integration [13] will provide bounded-error approximations of the joint kinematics.

A. Integrating Kinematics

As shown in (4), computing the link-to-link transformation $\mathbf{G}(\vec{q})$ reduces to the problem of solving an initial value problem for a LTV system on $[0, L]$,

$$\frac{d}{ds}\mathbf{G}(s,\vec{q}) = \mathbf{G}(s,\vec{q})\begin{bmatrix}\mathbf{\Omega}(s,\vec{q}) & \vec{v}(s)\\ 0_{1\times 3} & 0\end{bmatrix} \tag{18}$$

If the deformation of a sheet is confined to the case where $\theta(s) = 0$ everywhere (the Euler-Bernoulli bending case), then the problem is greatly simplified. In this case, the rotation of the hinge due to bending is planar and therefore commutative, so (1) can be solved explicitly for $\mathbf{R}(s)$ via the matrix exponential solution for first order homogeneous LTV systems. The Cartesian profile of the beam in (3) can then be solved by a numerical definite integration algorithm, such as Gauss-Legendre quadrature. The authors have previously shown that the planar case is accurate even when very low-order integration techniques are used [9].

In three dimensions, nothing about (18) can be solved explicitly, because the rotations along the backbone curve do not form a commutative subgroup. The whole equation must be solved numerically, by a time-stepping ODE solver such as Runge-Kutta, rather than a quadrature method. However, because the profile of the backbone curve is smooth, a low-order integrator with fairly large step sizes will suffice to accurately integrate the backbone profile. The authors used a second-order Runge-Kutta solver with a step size of $L/20$ to compute $\mathbf{G}(\vec{q})$.

B. Jacobian and Hessian Computation

To compute the Jacobian of some point on a robot with respect to the robot's generalized coordinates, the partial derivatives of the joint transformation with respect to any parameter q_i must be computed. The ODE describing this matrix, $\mathbf{G}_i(\vec{q})$, can be derived from (18), and are written here in compact form:

$$\frac{d\mathbf{G}_i}{ds} = \mathbf{G}_i\begin{bmatrix}\mathbf{\Omega} & \vec{v}\\ 0 & 0\end{bmatrix} + \mathbf{G}\begin{bmatrix}\mathbf{\Omega}_i & 0\\ 0 & 0\end{bmatrix} \tag{19}$$

All derivatives of $\mathbf{G}_i(\vec{q})$ are described by LTV systems of the same basic form as (18), having the same "A" matrix, and consequently the same state transition matrix for all values of i. As a result, much of the computation used to evaluate $\mathbf{G}(\vec{q})$ using a Runge-Kutta method can be reused to find $\mathbf{G}_i(\vec{q})$. Computing the Hessian of any point requires knowing the second partial derivatives of $\mathbf{G}(\vec{q})$, denoted $\mathbf{G}_{ij}(\vec{q})$. The ODE for the second partial derivatives, again derived from (18), also shares the same basic structure,

$$\begin{aligned}\frac{d\mathbf{G}_{ij}}{ds} = \mathbf{G}_{ij}\begin{bmatrix}\mathbf{\Omega} & \vec{v}\\ 0 & 0\end{bmatrix} + \mathbf{G}_i\begin{bmatrix}\mathbf{\Omega}_j & 0\\ 0 & 0\end{bmatrix} +\\ \mathbf{G}_j\begin{bmatrix}\mathbf{\Omega}_i & 0\\ 0 & 0\end{bmatrix} + \mathbf{G}\begin{bmatrix}\mathbf{\Omega}_{ij} & 0\\ 0 & 0\end{bmatrix}\end{aligned} \tag{20}$$

Thus, computation of the second partial derivatives of $\mathbf{G}(\vec{q})$ will reduce to solving the same underlying LTV system with different exogenous inputs, and can reuse much of the computation used for calculating $\mathbf{G}(\vec{q})$ and $\mathbf{G}_i(\vec{q})$.

C. Integrating Energy

Integrating the energy of a bending sheet numerically was performed with standard fixed-partition quadrature on the parameterized energy functional,

$$V(\vec{q}) = \frac{wh^3E}{12(1-\nu^2)}\int_0^L \kappa(s,\vec{q})^2 S\big(\gamma(s,\vec{q})\big)ds \tag{21}$$

An integration step size of $L/20$ was also found to be sufficient. While a fixed-partition method appears to work well, the possible divergence of $S(\gamma)$ is cause for concern. An adaptive step-size integrator may improve results if the joint is loaded tortuously, for example, with a large twisting moment. Because the energy is computed by integration on a fixed interval, the energy gradient (used by Castigliano's theorem to evaluate elastic forces on the joint) can be computed by taking the partial derivative of the integrand in (21) with respect to the joint parameters.

D. Summary

The low-dimensional basis of parameters used to describe the configuration of a bending sheet hinge can be mapped onto the joint's kinematic and energetic constitutive equation using fairly simple numerical integration methods. Due to the bounded and smooth nature of the sheet backbone curves, low-order integrators with large step sizes can be used. Most importantly, because the dimensionality of the parameter space is small, many of the adverse scaling issues often associated with modeling continuum systems using many finite elements will not be problematic under this smooth backbone model. Requiring some numerical integration is a small price to pay for avoiding the curse of dimensionality.

V. Implementation and Validation

The smooth backbone joint model was implemented by the authors in the Freeform Manipulator Analysis Toolbox, an

open-source, object-oriented Matlab library designed to flexibly prototype novel kinematic models of various kinds for manipulator analysis [14]. In order to examine the accuracy of the smooth backbone approach, deflection of a sheet hinge under load was computed for a range of off-axis loading conditions. Internal consistency of the model was evaluated by comparing the bending moment along the length of the hinge in two ways: first, by directly computing the moment arm at which the force was being exerted at any point s along the backbone curve, and second, by computing the internal elastic force resulting from the elastic deformation of the sheet. If the hinge shape is exactly at equilibrium, these two computations of torque should agree exactly. However, because the continuum model has been parameterized, some small errors will be seen. The magnitude of these errors and their implications for further model refinement will be discussed.

A. *In-Plane Loading*

When a sheet hinge is loaded by a force that is symmetric about the center of the joint, the resulting planar deflection is captured quite accurately. Figure 7 shows a the large-deformation equilibrium position of a beam of unitary length and bending stiffness, subjected to a unitary force offset by half the length of the beam on a rigid body. The point of force application is indicated by the arrow. The two nearly coincident curves plotted in Fig. 8 show that the prediction of moment along the backbone from the kinematics of the solution, that is, $\tau_k = (\vec{x}(s) - \vec{p}) \times \vec{F}$, agrees with the prediction of moment based on elastic forces, $\tau_e = EI\kappa(s)$ to within 0.35% of the normalized unitary moment, or a moment of PL/EI for a beam with arbitrary length, loading force and stiffness. This means that despite considering only the modal balance of forces on the beam, the local balance of forces everywhere are more or less in equilibrium.

B. *Three-Dimensional Loading*

The same sheet, having an aspect ratio $w/L = 2$, was then loaded by a force offset from the centerline of the hinge by a distance a, as shown in Fig. 9, so that twisting as well as bending motion resulted. Because the axis of bending is skewed by the three-dimensional motion of the sheet, the moment arm was calculated by finding the normal distance from the line of applied force, the elastic moment was computed including the shape factor, $\tau_e = EI\kappa(s)S(\gamma)$. The two predicted moment profiles are plotted in Fig. 10 for a lateral offset $a = 2L$, and the agreement between the two profiles is poorer than the planar case, especially at the two ends of the sheet. The peak absolute errors between the kinematic moment τ_k and the elastic moment τ_e for a range of offsets are shown in Fig. 11, and in each case, the error peaks occurred at or near the ends of the sheet.

C. *Discussion*

Errors in moment profile are not positional errors, but they do give a sense of the fidelity of the smooth backbone model for sheet hinges. The results shown in Fig. 10 indicate that the mode shapes chosen here to model the axis of bending in

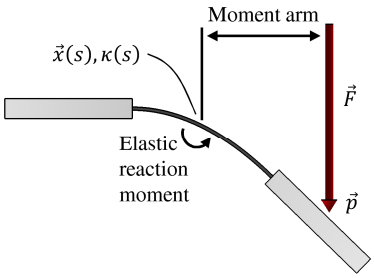

Fig. 7. An approximate bending model can be validated by comparing the elastic reaction moment of the flexure based on its shape to the moment as calculated by the moment arm from the axis of bending to the line of applied force.

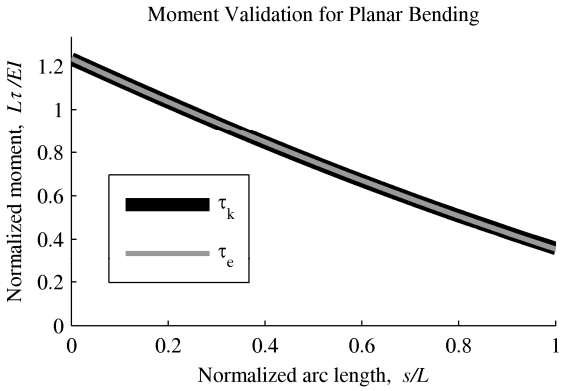

Fig. 8. For the planar case of the smooth backbone sheet model, the agreement between the elastic moment prediction and the kinematic moment prediction is very close, within 0.35%.

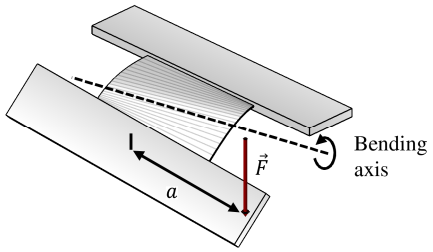

Fig. 9. A lateral offset a was applied to the end load, and the resulting deformation was calculated.

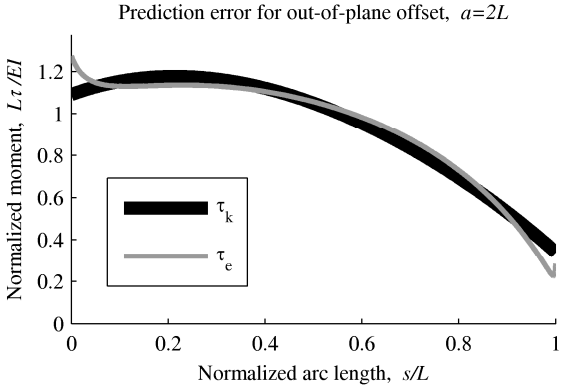

Fig. 10. The prediction error for a maximum lateral offset of $2L$. The error in the moment profile is mainly concentrated around the two ends of the hinge.

a flexible sheet produce on average accurate reaction forces over the length of the hinge, but tend to make the edges of the sheet a little stiffer or more compliant than they actually are. This is a likely consequence of the strong effects of the end conditions of the sheet on the overall shape. It is quite possible that a set of nonlinear mode shapes for angular profile taking into account factors such as the aspect ratio of the hinge could improve substantially on this result. Overall, the ability to represent both gross bending and twisting motion of the joint in response to an off-centered load is encouraging. Future work will focus on refining the mode shapes for bending profiles and comparisons of deflection accuracy to known good models of ruled surface bending.

VI. Conclusion

Creative mechanism selection has always been a driving force for innovation in robotics; this often means using mechanisms like sheet hinges whose behavior is difficult to capture in models that are convenient for robot design, analysis, and control. The model presented in this paper is one attempt at addressing this gap between mechanisms and models in a way that can hopefully be integrated into any rigid body modeling software tool. Low-dimensional models which present a clean interface to both the kinematics and the elastic energy of non-traditional joints will ultimately enable a wider array of robots to be considered as first-class citizens in the domain of robot modeling and control.

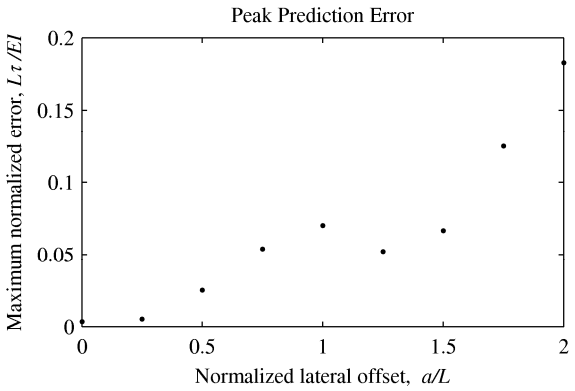

Fig. 11. The peak absolute moment prediction errors observed in a flexure hinge with an offset applied load. These errors were concentrated around the end of the sheet and

References

[1] E. Smela, Olle Inganäs, and Ingemar Lundström, "Controlled folding of micrometer-size structures," *Science*, 268 (23 June), 1735-1738, 1995.

[2] E. Hawkes, B. An, N. Benbernou, H. Tanaka, S. Kim, E.D. Demaine, D. Rus, and R.J. Wood, "Programmable matter by folding," Proc. Nat. Acad. Sci., 107 (28), pp. 12441-12445, 2010.

[3] J.P. Whitney and R.J. Wood, "Aeromechanics of passive rotation in flapping flight," J. Fluid Mechanics, v. 660, pp. 197-220, 2010.

[4] F. Lotti, P. Tiezzi,G. Vassura, L. Biagiotti, C. Melchiorri, "UBH 3: An Anthropomorphic Hand With Simplified Endo-Skeletal Structure and Soft Continuous Fingerpads," IEEE International Conference on Robotics and Automation, ICRA '04, New Orleans, 2004.

[5] A. M. Dollar and R. D. Howe, "The Highly Adaptive SDM Hand: Design and Performance Evaluation," International Journal of Robotics Research, Vol. 29, No. 5, pp 585-597, 2010.

[6] E. Bayo, "A finite-element approach to control the end-point motion of a single-link flexible robot," Journal of Robotic Systems, vol. 4(1), pp. 63-75, 1986.

[7] A. Midha, T. Norton, and L. Howell, "On the nomenclature, classification, and abstractions of compliant mechanisms," Trans. of the ASME, v. 116, n. 1, pp.270-280, 1994

[8] H. Su, "A pseudorigid-body 3R model for determining large deflection of cantilever beams subject to tip loads," ASME J. Mechanisms and Robotics, v. 1, p. 021008-1

[9] L. Odhner and A. Dollar, "The smooth curvature flexure model: an accurate, low-dimensional approach for robot analysis," in *Robotics: Science and Systems 2010*, MIT Press, 2010.

[10] P. F. Pai, A. N. Palazotto, "Large-deformation analysis of flexible beams," International Journal of Solids and Structures, v. 33, n. 9, pp. 1335-1353, 1006.

[11] L. Mahadevan and J.B. Keller, "The Shape of a Mobius Band," Proc. R. Soc. London, v. 440, pp. 149-162, 1993.

[12] R. Murray Z. Li S. Sastry, *A Mathematical Introduction to Manipulation*. ch. 7.2, CRC Press, 1994.

[13] W. Press, S. Teukolsky, W. Vetterling, and B. Flannery, *Numerical Recipes in C*, 2nd ed., Cambridge University Press, 1992.

[14] L. Odhner and A. Dollar, "The Freeform Manipulator Analysis Toolbox" [Online]. Available http://www.eng.yale.edu/grablab/fmat/